Subsurface site characterization of Donga Fan, Northwest Himalaya using multichannel analysis of surface waves and response analysis

Ambrish Kumar Mahajan[1,2,*] **and Praveen Kumar**[2]

[1]Wadia Institute of Himalayan Geology, 33, GMS Road, Dehradun 176 215, India
[2]Central University of Himachal Pradesh, Dharamshala 176 215, India

The characterization of sediments in a tectonically complex region is important from the seismological point of view to study possible earthquake effects due to the presence of soft sediments. Multichannel analysis of surface waves (MASW) method was used to acquire seismic data from 87 sites for estimating shear wave velocity (V_s) of near-surface materials beneath the Donga Fan. The majority of the Donga Fan is underlain either by alluvial fan or river terrace deposit. About 80% of the Donga Fan has an average shear wave velocity ranging from 180 to 360 m/s, whereas 20% of the area has high stiffness values ($V_s \geqslant 360$ m/s). The estimated V_s values are higher in the northern part of the study area due to thin sediment (<30 m) cover compared to the central, south and southwestern parts which have thick sedimentation (>150 m) above bedrock. The response analysis suggests that peak spectral acceleration varies from 0.49 *g* at 1.61 Hz to 1.69 *g* at 3.22 Hz with variation in amplification ratio from 4 to 11 times. The spectral acceleration computed for two-storey buildings also varies from 0.10 to 0.40 *g* (at 5% damping), whereas in the case of single-storey buildings it varies from 0.12 to 0.22 *g* (at 5% damping). The predominant frequency estimated using ambient noise measurements varies from 0.84 to 5 Hz, indicating variation in the thickness of sediments and is in good agreement with the V_s values estimated using the MASW technique.

Keywords: Bedrock response analysis, multichannel analysis of surface waves, site response, shear wave velocity.

ALL along the Himalayan frontal belt, a number of intermontane, broad and open synclinal valleys or Dun basins dominate the morphotectonic features of the sub-Himalaya, e.g. Ropar-Pinjor Dun and Dehra Dun (Doon) in the Northwest Himalaya having thick sedimentary cover[1] (Figure 1).

The Dehradun basin or Doon Valley is one such basin which is further characterized by the presence of three major fans, i.e. Donga Fan, Dehradun Fan and Bhogpur Fan. The Donga Fan is located to the west of the Dehradun Fan and has thick erosional deposits. On the seismic hazard map of India[2], this valley falls in the second highest hazard category (zones IV and V) with occurrence of major and moderate earthquakes, namely the 1905 Kangra (7.8 Ms), Uttarakashi (6.8 Mw) and 1999 Chamoli (6.4 mb) earthquakes during the last century[3–6]. The seismicity maps of the NW Himalayan region prepared using recently updated earthquake data show that the

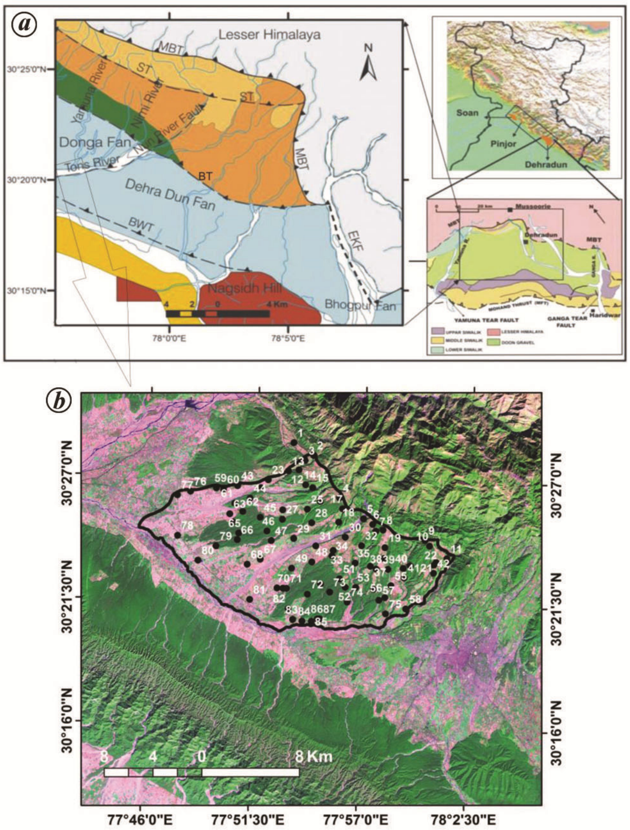

Figure 1. ***a***, Map showing geology and tectonic elements of Doon Valley, India, covering Donga, Dehradun and adjoining fans. MBT, Main Boundary Thrust; MFT, Main Frontal Thrust, ST, Santaurgarh Thrust; BT, Bhauwala Thrust; BWT, Bansiwala Thrust; NRF, Nun River Fault; EKF, East Kalinga Fault; LH, Lesser Himalaya; US, Upper Siwalik; MS, Middle Siwalik. (Inset) Locations of three Duns in Northwest Himalaya, India and on the regional tectonic map of Doon Valley[1]. ***b***, Locations of sites covered beneath Donga Fan in the backdrop of Landsat image showing physiographic features.

*For correspondence. (e-mail: akmahajan@rediffmail.com)

study area is bounded by high hazard potential seismogenic zones, i.e. Kangra seismogenic zone to the west, and Uttarakashi and Chamoli seismogenic zones to the northeast and eastern regions respectively (Figure 2). Active tectonics, seismic hazards and palaeo-seismic studies have also indicated that the area is situated in a region with high seismic 46 hazard potential[1,6–9].

The area immediately to the west of Doon Valley is the southeastern Himachal Pradesh (Shimla) region, which has been considered as the seismic gap region as it has a very low seismicity rate since the last 100 and 500 years. Considering the seismic gaps of Eastern Himachal[10] and other seismic gap regions all along the Himalayan arc, it may not be equally seismogenic to generate great earthquakes[11,12]. Thus the Himalayan arc is found to be segmented in nature and there are significant variations in the strain values of different segments based on seismicity for the last 500 years[13]. Further analysis indicated that the southeastern Himachal Pradesh (Shimla) region has a clear deficit in seismic energy release even after considering the last 100 years of earthquake data. Although this region does not fulfil the criteria for generating great earthquakes, large or moderate earthquakes cannot be ruled out. If this region gets activated any time, the Donga Fan which is close to it will experience a much larger effect due to strong excitation from the southeastern Himachal Pradesh, Uttarakashi and Chamoli regions. Thus, the Donga Fan falls under high hazard zone due to the presence of difference seismogenic zones around it.

Under such conditions the study of site amplification is significant because the southern part of the Fan has a thick sedimentary cover with soft soil or very thin soft soil above bedrock in the northern part. Considering the high hazard potential, increasing asset value and population growth unconstrained by building codes requires characterizing each site in terms of site amplification, which is currently an important tool for assessing seismic

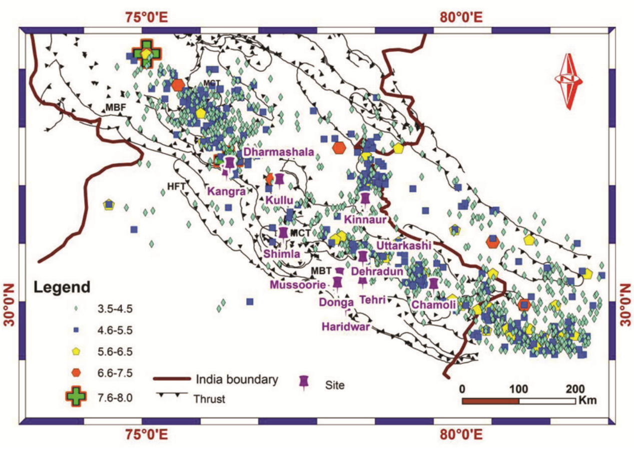

Figure 2. Seismotectonic map of NW Himalaya showing zones with high seismic potential around Donga Fan. (Earthquake data from 1900 to 2018. Source: ISC Bulletins for magnitude range $M > 4.0$.)

hazard at regional and local scale[14]. The presence of active faults in and around the Donga Fan can also increase the seismic hazard potential of the region[15]. The Donga Fan area had a scanty population with poorly built earthquake non-resistant structures (adobe and burnt brick houses) before the formation of Uttarakhand state (November 2000). Later, the area was earmarked for setting up educational institutions and industries. The extent and spate of damage observed during the 2015 Nepal earthquake (7.6 Ms) to the poorly constructed structure and buildings raised challenging questions about risk management and the responsibility of disaster managers to reduce the ensuing disaster from future earthquakes. The development for economic growth of the country, the Donga Fan which is contributing towards the development of the nation requires an estimation of site amplification parameters.

Shear wave velocity (V_s) along with density of the material are key parameters in estimating the site response of any sedimentary basin soil[16]. Presently, the engineering community is using the shear wave velocity for designing structures[17].

In India we are still in a process of measuring shear wave velocity of the earthquake-prone regions. Although some cities have been covered under seismic microzonation studies, like Dehradun, Sikkim, Jammu and NCR Delhi, several urban centres of the frontal Himalayan region need to be studied for collecting such data, which are located in a very high hazard zones and fall under seismic zones V and IV (ref. 2). In this study, a newly coming up urban centre of Doon Valley (Donga Fan) has been considered. The Ministry of Earth Sciences, Government of India (GoI) is encouraging seismic microzonation studies of major urban centres in the near future. The estimation of hazard of any urban centre requires rapid and inexpensive measurements of shear wave velocity over large sedimentary cover for accurate estimation of future hazard maps. Traditionally, standard penetration test is used for the estimation of V_s parameters, especially for site-specific projects. However, for the estimation of V_s parameters over large sedimentary cover, a multichannel analysis of surface waves (MASW) method has been used which has also been validated with the results obtained through microtremor measurements carried out in open and heavily urbanized areas[18,19]. Although the ambient noise measurements have limited spatio-temporal resolution for the near-surface materials, the MASW method has been used for high resolution of the near-surface materials[17]. The MASW method has been developed more recently for determining shallow V_s (ref. 18) and is extensively used in major urban centres of the NW Himalaya[19,20].

In complex geological settings like that of the present study area where there are irregular variations in stiffness and high impedance contrast between the bedrock and unconsolidated sediments, the data acquired using the

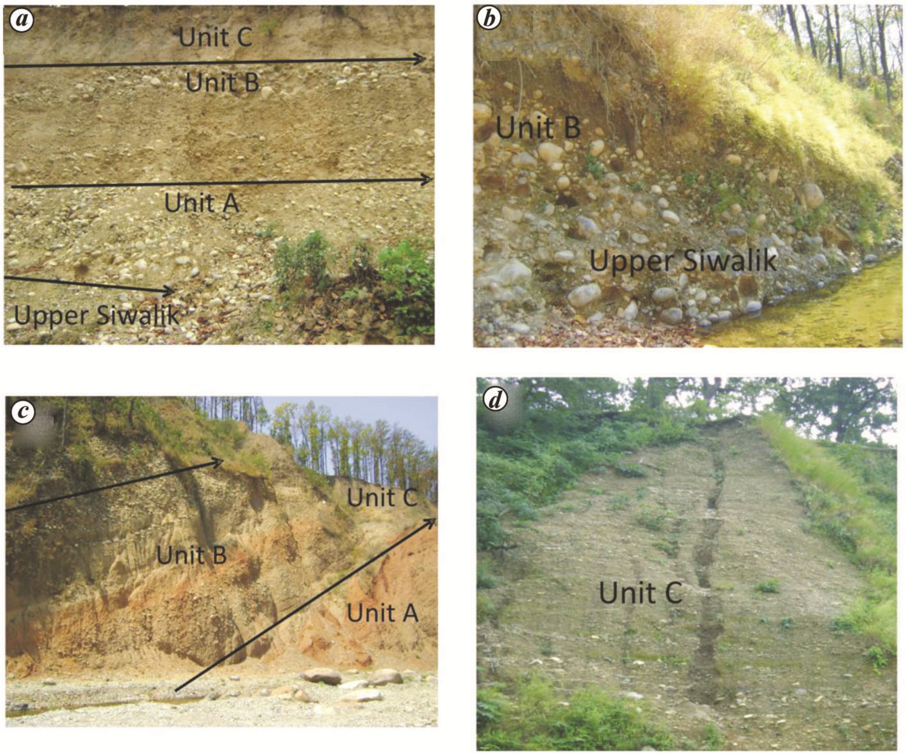

Figure 3. Different litho-units of post-Siwalik Doon gravels under the Donga Fan. ***a***, Section exposed along Nimi Nadi from Kandoli site at the northern part of the Fan showing different units of Doon Gravels. ***b***, Section exposed in Majhaun site. Above this section, shear wave velocity profiles have been taken to validate the shear wave velocity profiles with depth. ***c***, Section showing different litho-units of Doon Gravels located close to Majhaun site (site no. 40) river section. ***d***, Close view of unit C exposed at the southern part of the Fan (site no. 81). The classification proposed by Thakur and Pandey[1] has been adopted.

MASW method require attention during processing and inversion[18].

Geological and geomorphic setting

Tectonically, the Doon Valley is sandwiched between two major thrusts, i.e. the Main Boundary Thrust (MBT) to the north and the Main Frontal Thrust (locally named as Mohand Thrust) to the south, and comprises mainly Doon Gravels. Litho-stratigraphically, the Doon Gravels are the resultant of post-Siwalik depositions, and the active tectonic activity coupled with tropical climate and monsoon rainfall control the deposition and erosion of Fan sediments[21]. In the piedmont area, the Donga Fan is unconformably deposited over eroded and steeply dipping Middle Siwalik rocks having very thin alluvial cover (20–30 m)[1]. The Middle Siwalik rocks (sandstone) are also exposed in the central part of the Fan along stream sections[21] (Figure 1). The Doon Gravels are massive, thickly bedded and poorly consolidated to unconsolidated conglomerates (comprising pebbles and boulders in a fine-grained matrix; Figure 3 *a* and *c*).

The northern part of the Fan is also characterized by dissecting Doon Gravels with lime-enriched materials, which acted as the cementing material in gravel beds thus increasing the stiffness of the sediments. The Doon Gravels can be divided into three major units[1]: A–C. Unit A lies over the steeply dipping sandstone of Middle Siwalik rocks and comprise sub-angular to sub-rounded granule to pebble-sized clasts set in fine-grained matrix, thus forming a very stiff soil, whereas unit B unconformably overlies on unit A, and at some places it directly overlies on the Middle and Upper Siwalik Formations. These relationships have been observed under Donga Fan area (Figure 3 *b*). Unit B consists of unconsolidated massive gravels with predominance of rounded to sub-rounded boulders, which unconformably overlie on the Upper Siwalik Conglomerates. The gravels are poorly sorted and clast-supported in the northern part, whereas these are matrix-supported in the southern part of the Fan (Figure 3 *a*, *c* and *d*). Unit C is a younger Fan surface which has unconformable contact with both units A and B and the Siwalik Formation (Figure 3 *a* and *c*) in the northern part of the Fan area. This unit predominantly comprises poorly sorted angular to sub-angular granules and pebbles that are interspersed with boulders (Figure 3 *d*). The clasts are supported by a gritty matrix, whereas boulders and pebbles are set in with finer clast matrix. The distal part of the Fan area is rich in clay content with the decrease in clast size, mud and silt, thereby making the topsoil usable for brick kiln industry.

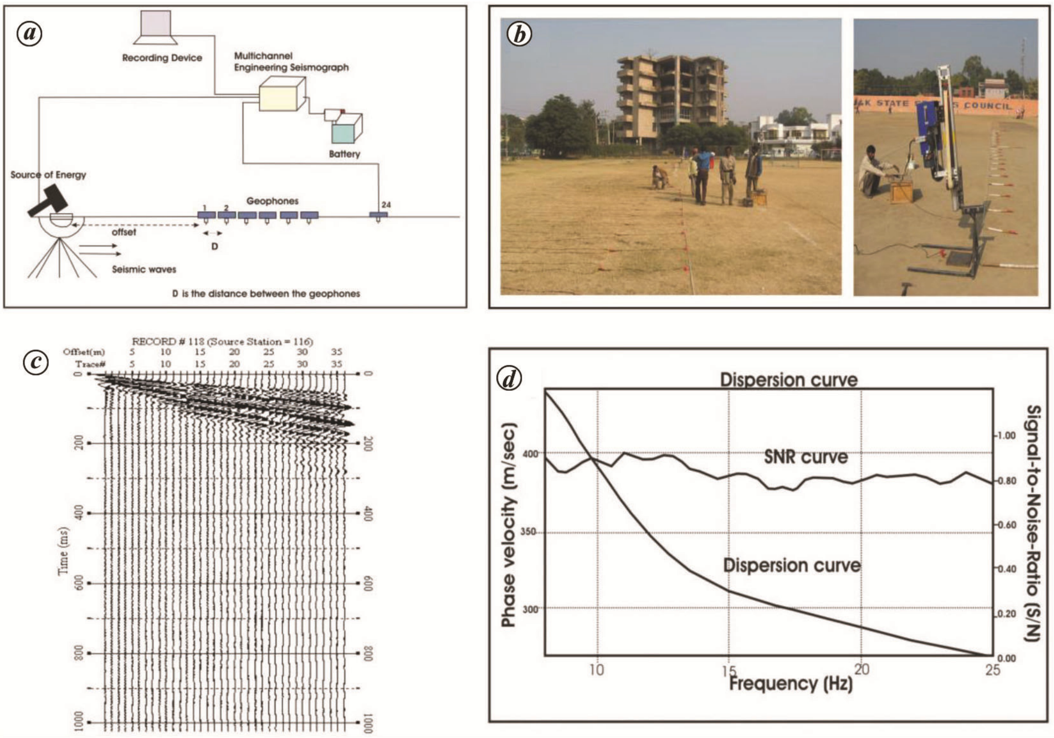

Figure 4. Schematic diagram showing field configuration of Multichannel Analysis of Surface Waves (MASW). ***a***, Different components used in the MASW survey. ***b***, Layout of geophones on a survey line with 40 kg accelerated weight drop hammer as an impact source. ***c***, Shot gathered and combined in one single trace using walkaway method. ***d***, Extraction of dispersion curve for 1D shear wave velocity inversion.

Data acquisition and analysis

The shear wave velocity of the Donga Fan was estimated using MASW method. This is a non-destructive seismic method that inverts V_s profiles of the subsurface from the dispersive property of Rayleigh waves[18,19,22,23]. The Rayleigh waves, normally known as ground roll, have low velocity, low frequency but high amplification in soft sediments[22,23]. Continuous acquisition of multichannel surface wave data along a linear transect generates two-dimensional (2D) V_s profiles having a total spread length of ~72–100 m that contains information about the horizontal and vertical continuity of materials as shallow as 30–100 m. The data have been acquired from 87 sites using 24-channel seismograph with 4.5 Hz spike-based vertical geophones. The seismic source used is a propelled energy generator (PEG-40 kg), which is an elastometer aided weight drop hammer (EAWDH). The shear wave velocity data have been retrieved using geophone interspacing of 1 m (Figure 4 *a* and *b*).

The receiver spacing and offset distance were decided after optimizing the field parameters by experimenting at different sites over the Donga Fan, which vary from 1 m (near shot) to 25 m (far shot). The data were collected by moving both source and receiver in an incremental manner using roll along method for conducting 2D shear wave velocity profiling, thus covers total spread of 73–97 m. At each shooting location, multiple stacks (10–15) were made to enhance the signal and obtain good resolution of the dispersion image in active MASW survey[22–24]. The depth of investigation in this technique depends on various parameters, i.e. elastic properties, density of the soil/rock, seismic source, frequency of the geophone and spread length[22,23,25]. The available equipment in combination with the used parameters eventually produced sections with an investigation depth ranging from 30 to 60 m. A record length of 1.024 sec with a sampling rate of 0.5 ms was found to provide good quality records[19,20]. On the other hand, in order to cover maximum areas, one-dimensional (1D) profiling was also done along a linear transect using the source at different offset distances (20, 40 and 60 m) having geophone interspacing of 1 m (Figure 4 *b*).

The data processing was performed using SurfSeis 3.0 software, which includes conversion of SEG-2 data to KGS format, assigning the field geometry to the acquired data. Shots gathered from the near (1 m), middle (13 m), and far offset (25 m) of the survey line were configured with field parameters to generate seismic records for each shot using the walkaway method (Figure 4 *c*). Each seismic record was then processed using preliminary parameters to obtain overtone image in order to select reference phase velocity and phase frequency. The amplitude of the signal is represented by colour variation in the overtone image, which otherwise demonstrates whether the mode considered is correctly selected for the specific type of

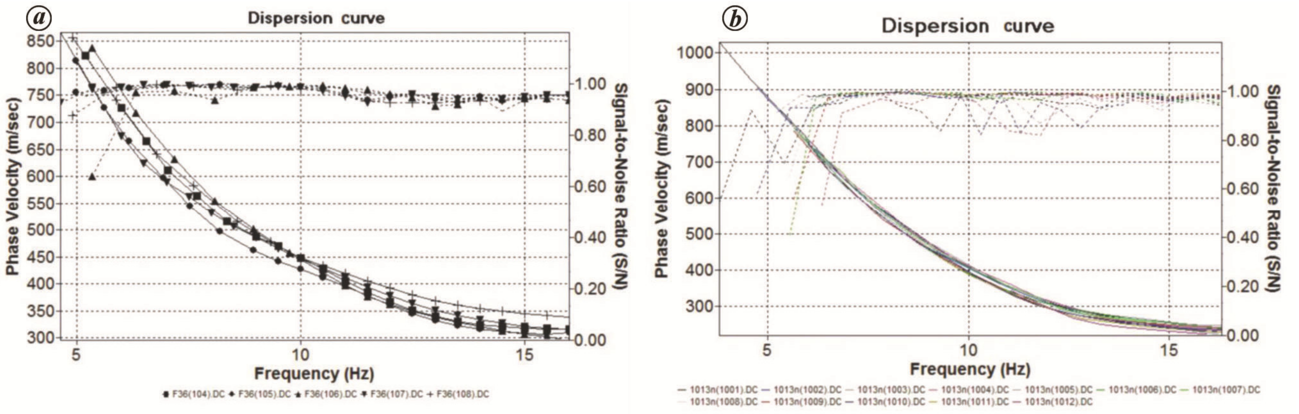

Figure 5. Multiple dispersion curves derived from two sites, i.e. (***a***) Kandoli and (***b***) Badowala from the Donga Fan area. The overlapping of dispersion curves from different shooting locations indicates the reliability of results as all the dispersion curves show similar trend.

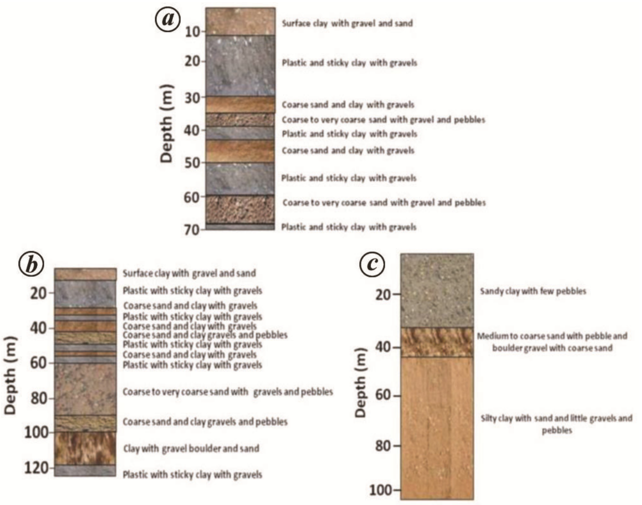

Figure 6. Litho-sections obtained from the borehole data. ***a***, Chhorba (site no. 63). ***b***, Baluwala site (site no. 76). ***c***, ICFAI University Campus (site no. 81).

inversion applied or not. The dispersion analysis was then performed using each overtone image by normalization of complex numbers with Fourier transform[19,22,23] (Figure 4 *d*). In order to increase the confidence level in our dataset, a number of dispersion curves were plotted with their corresponding signal-to-noise ratio (SNR) using different shooting locations from the same site. Figure 5 shows the reliability and consistency of the results. As observed from Figure 5, SNR remains above 0.8. The reason for forming the 2D analysis is to determine the vertical and lateral variabilities under the Donga Fan.

In the present analysis, phase velocity of 850–1000 m/s were observed at frequencies as low as 3–4 Hz, and phase velocity of 200 m/s at frequencies of 10–15 Hz, thus indicating the depth of investigation achieved. Since wavelength (λ) is a function of phase velocity (c) as well as frequency (f), it is possible to obtain information at depth down to 10–100 m (Figure 5). However, the 1D shear wave velocity profile shows an investigation depth >100 m when the shooting offset distance is 40–60 m and accelerated weight drop as an impact source is being used.

Results and discussion

Validation of shear wave velocity profiles

In order to constraint the shear wave velocity profile, independent information is needed. The stratigraphic information obtained from geotechnical studies carried out in Doon Valley[26] and lithological information from borehole data provided by the Ground Water Board, GoI have been used. Most of the borehole information was drilled through Doon Gravels and the corresponding lithology is shown in Figure 6 for three sites along with a description of the materials mapped in the litholog profile.

The sites considered for validation in the present study are Chhorba (site no. 63), Baluwala (site no. 76) and Institute of Chartered Financial Analysts of India (ICFAI) University, Campus (site no. 81) from the western, central and southeastern parts of the Fans respectively (Figure 7). The Chhorba site is famous for brick kiln industry, and the top 15 m soil shows clay and sand. The shear wave velocity of the top 15 m soil cover is 160–200 m/s from the 2D profiles, indicating a very soft soil according to the National Earthquake Hazard Reduction Programme (NEHRP) soil class (Figure 7 *a*). Below 15 m depth the soil is marked by the presence of plastic and sticky clay with gravels, thus increasing the shear wave velocity to 300–400 m/s up to 40 m depth. Below 40 m depth, the soil column shows alternating layers of coarse sand with clay and gravel and plastic sticky clay with gravel, thus representing a shear wave velocity of 550–600 m/s and can be classified as unit C (ref. 1).

The second site reveals that the top 20 m of soil has the same velocity as the top 12 m of Chhorba site followed by a second layer of 40–45 m thickness with V_s of 300–400 m/s. The last layer shows alternating coarse sand and clay with gravel at a depth of 60 m with a shear wave velocity of 550–700 m/s, thus representing lateral variation in stiffness (Figure 7 *b*). The last site validated was the ICFAI University Campus where a funnel-shaped feature with depth suggested that there is a decrease in velocity in the central part compared to the extreme ends of the profile indicating attenuation of shear wave velocity, thus inferred as presence of water-bearing beds. The first layer of this site also have very low shear wave velocity (160–200 m/s), but the thickness of this layer goes up to ~30–40 m with lateral variation (Figure 7 *c*). The second layer (~30–70 m) shows presence of coarse sand, clay and gravel, thus representing the same shear wave velocity as of Baluwala and Chhorba site (site no. 63). The shear wave velocity variation with depth at different sites may indicate depositional environment.

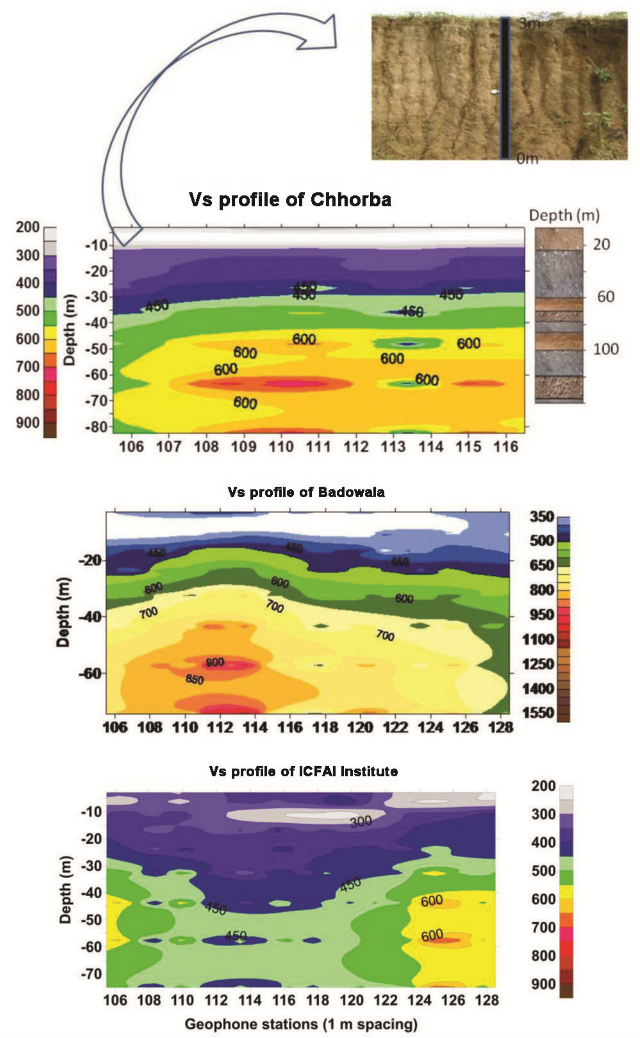

Figure 7. Shear wave velocity profiles of three sites. (***a***) Chhorba (site no. 63). (***b***) Baluwala (site no. 76) and (***c***) ICFAI University Campus (site no. 81). The inference on material composition is also confirmed by the litholog of the respective sites.

The 2D shear wave velocity profiles derived from the northern part of the Fan using the MASW technique have also been validated using litho-sections of the Donga site (site no. 5) and Majahun site (site no. 40) located within the Donga Fan[20], where bedrock (sandstone) is exposed at very shallow depth along the river section. It is important to mention that the shear wave velocity is not an analogy to the lithology, as it depends on the volumetric fracture density, rock fabrics (e.g. shear wave splitting), overburden thickness and water content, among others and is therefore not uniquely correlative with lithology, but provides stiffness of the soil. Based on the NEHRP Classification[27], materials having $V_s > 760$ m/s are considered as rocks for engineering applications. Thus running seismic profile directly over the exposed litho-sections will provide shear wave velocity values of bedrock and other lithologies, which enable us to correlate them for the unexposed section (Figure 3).

The shear wave velocity estimation was conducted covering 87 sites from the Donga Fan. The average shear wave velocity of the northern part of the Fan area was higher than the central and southern parts. The shear wave velocity of sites nos 1, 3, 5, 8, 24 and 39 (Tauli Langa, Pipalsar, Donga, Bidholi, Kandoli and Gadaria sites respectively; Figure 1) varied from 300 m/s at the top few metres to about 500 m/s up to 15–20 m, and increased up to 850 m/s below 30 m depth. The high V_s values at a depth of 30 m reflect the velocity of engineering bedrock level which may represent shear wave velocity of the underlying Siwalik rocks (Figure 8 *a*).

The low root mean square error (RMSE) values suggest a high level of confidence (Figure 8 *b*). The RMSE is calculated based on the V_s profile of a layer whose theoretical dispersion curve shows the best match with the

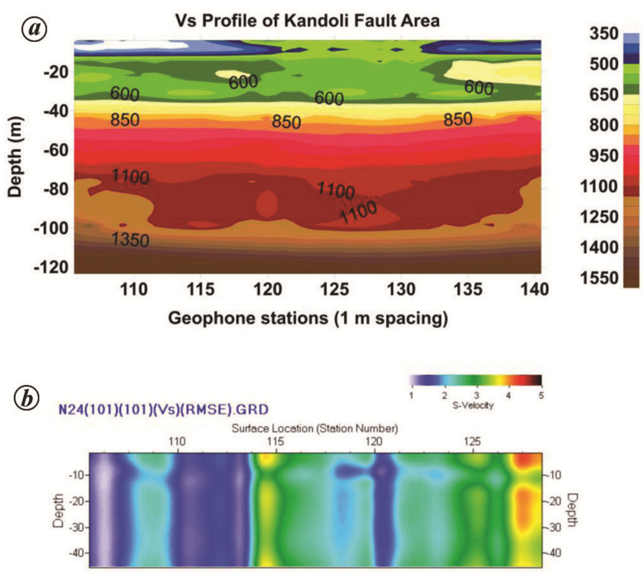

Figure 8. ***a***, Two-dimensional shear wave velocity of Kandoli site (site no. 39). ***b***, The respective root mean square error (RMSE) profile.

calculated dispersion curve using RMSE as a guide and constraint. RMSE is a measure of relative error for each layer in comparison to theoretical criteria, and can be used as a measure of confidence[18].

Sites like Badowala (site no. 33), Chandpur Khurd (site no. 45), Bhagwanpur (site no. 38), Manduwala (site no. 52), Dhakoliwala (site no. 53), Silver Heights (site no. 56), Kedarwala (site no. 60) and Bahadarpur (site no. 69) show low shear wave velocity (200–300 m/s) for the top 15–20 m soil cover, followed by V_s of 400–500 m/s for the next 10–15 m soil column, indicating stiff soil behaviour of the top 30 m soil column. The shear wave velocity increased to >700 m/s below 40–45 m depth (Figure 9 *a*). In general, the shear wave velocity increases with depth with slight variation in the surrounding may be due to presence of water bearing bodies.

On the other hand, sites like Badowala and Chandpur Khurd located adjacent to the river beds show very low velocity in the top 15–20 m soil cover which varies from 160 to 200 m/s, followed by 300–400 m/s for next 20 m depth (Figure 9 *b*). Further below at 40 m depth, V_s increases to 800 m/s. However, at the eastern end of the section below, the station location 122–126, the shear wave velocity drops to 450–500 m/s compared to the surrounding sediments. Thus, it may indicate the presence of dissolution features or moisture content below 40 m depth.

The southern part of the Fan shows a very thick layer of clay (Figure 10). The clay is found to be much stiffer if it is dry; however, it has very less stiffness under moist conditions. Most of these sites are used for making burnt bricks. The top 20 m soil column has low shear wave velocity (350–400 m/s) and below the location of stations 135–140, the same velocity is extended up to 60 m depth. Thus, it may indicate the presence of moisture or water content at Rajawala site (site no. 49). Similarly, the shear wave velocity profile of Dhoolkot site (site no. 72) up to 40 m depth is between 350 and 400 m/s (Figure 10). The shear wave velocity derived for different sites of the Fan shows that the topsoil has velocity ranging from 300 to 400 m/s (5–12 m only) in the northern part, 200–250 m/s (10 m) in the central part and <200 m/s (10–20 m) in the distal part of the Fan. The second layer has a shear wave velocity of 500–600 m/s (12–18 m depth) in the northern part of the fan, 300–400 m/s (10–22 m depth) in the central part and 250–350 m/s (20–25 m depth) in the distal part. The third layer has a shear wave velocity of >760 m/s (below 18–20 m depth) in the northern part of the Fan, 500–600 m/s (22–40 m depth) in the central part of the Fan and 400–550 m/s below 25 m depth. The isolated high below the location of station 112 is stiffer (may be due to gravels) compared to its surrounding profile. The study carried out for Dehradun Fan sediments complements the observations made in the Donga Fan area[28].

Based on the information from 2D shear wave velocity profiles and SHAKE 2000 (ref. 29) analysis the average shear wave velocity along with other parameters like natural frequency of the soil column, response spectra and amplification spectra have been derived. The average shear wave velocity, depth to bedrock and response parameters and amplification ratios have been tabulated

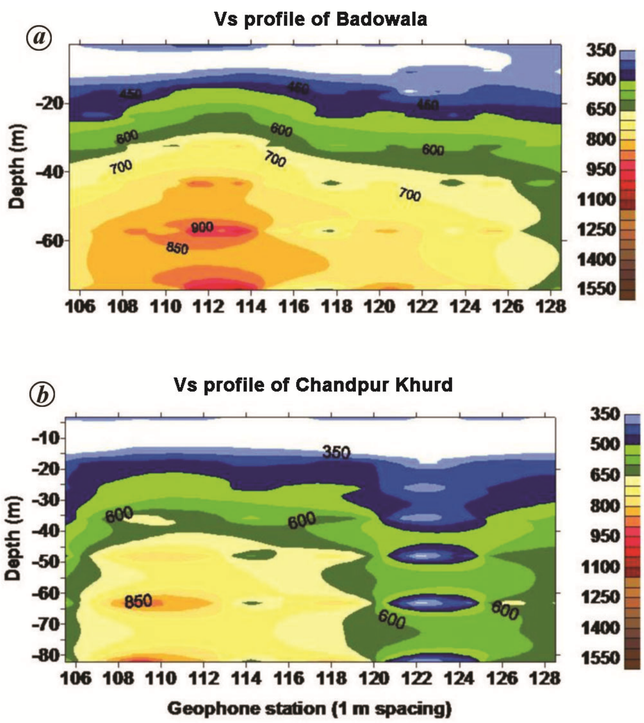

Figure 9. Shear wave velocity profiles of Badowala (site no. 33) and Chandpur Khurd (site no. 45) indicating the lateral and vertical variation at different sites of the Donga Fan.

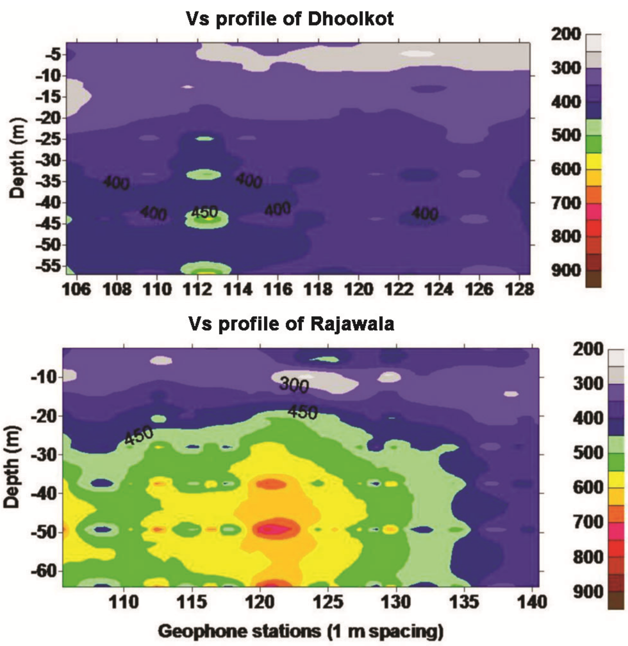

Figure 10. Shear wave velocity profiles of Dhoolkot and Rajewala sites (site nos 72 and 49) indicating vertical variation.

in attribute table along with site location maps for visualization. All point information was then interpolated considering average distance between points and the survey profile line. The interpolation of all spatial data was performed in Arc View and Arc GIS software with a grid spacing of 25 × 25 m. The interpolated values were classified based on the natural grouping of data to produce a number of classes. According to NEHRP classification, different classes have been defined for the shear wave velocity map. The shear wave velocity values were then contoured using krigging method to generate a V_s map. Figures 8–10 show the variation of shear wave velocity with depth, indicating that the northern part of the Fan has stiffer soil compared to central and distal parts. Based on the NEHRP classification[27], the Donga Fan has been classified into three soil classes, i.e. C (V_s = 360–760 m/s), D (V_s = 180–360 m/s) and E (V_s = 180 m/s). Of this, 80% of the area fall under class D (Figure 11).

Response analysis

According to the shear wave velocity estimation, it can be concluded that the thickness of sediments above engineering bedrock in the northern side of the Fan is about 10–20 m; however, near the MBT, the engineering bedrock (V_s > 760 m/s) is exposed at the surface. All along the river section downstream, several river terraces have been developed by these streams, and the thickness of sediments in these terraces above engineering bedrock was found to be within 20–25 m. The total thickness of the sediments was found to be >50–100 m in the middle of the Fan area and >150–200 m in the distal part of the Fan (Figure 12).

The thickness of sediments and shear wave velocity are the main parameters which affect the amplitude, frequency and duration of vibration that in turn determine the severity of hazard in any area. More importantly, seismic methods are dependent upon stress and strain behaviour; so the subsurface deposits with large contrast in density and velocity can bring spatial variability of the damaging pattern under fan deposits. However, the Donga Fan deposits do not have much variation in density of the material as all the sediments have been derived from the same source (adjoining Lesser Himalayan and Outer Himalayan rocks). However, the near-surface material properties, i.e. stiffness, damping of the material and impedance contrast play a major role in site amplification of different sites in the Donga Fan. Shear wave velocity is one the key parameters in controlling the damage pattern of any region, and is assumed to propagate vertically upwards from the bedrock and their motion will be different for outcrop and at near surface; so their transfer function has been approximated using linear computer algorithm SHAKE2000 (ref. 29). Since the shear wave velocity was acquired using low strain source, strong ground motion {Chamoli earthquake (6.4 mb) with PGA as 0.054 *g* for bedrock} from the region was taken as the

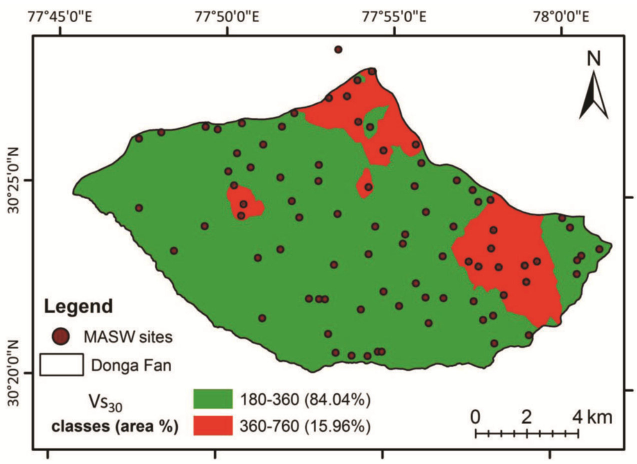

Figure 11. Average shear wave velocity map of the Donga Fan.

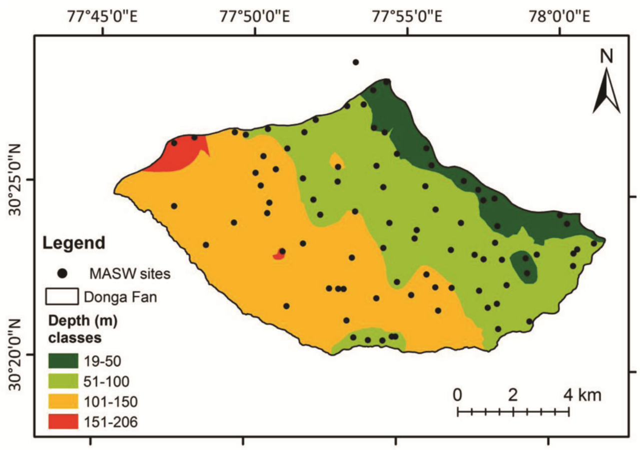

Figure 12. Thickness of sediments above engineering bedrock beneath the Donga Fan.

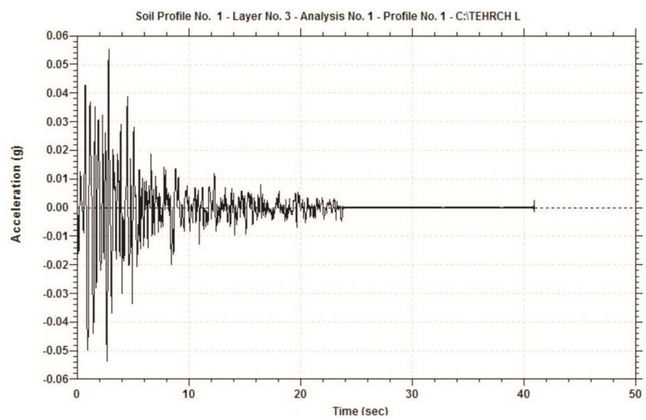

Figure 13. Computed acceleration time history for Kandoli site using SHAKE2000 from horizontal component strong motion data of the Chamoli earthquake. (Source: Department of Earthquake Engineering, Indian Institute of Technology, Roorkee.)

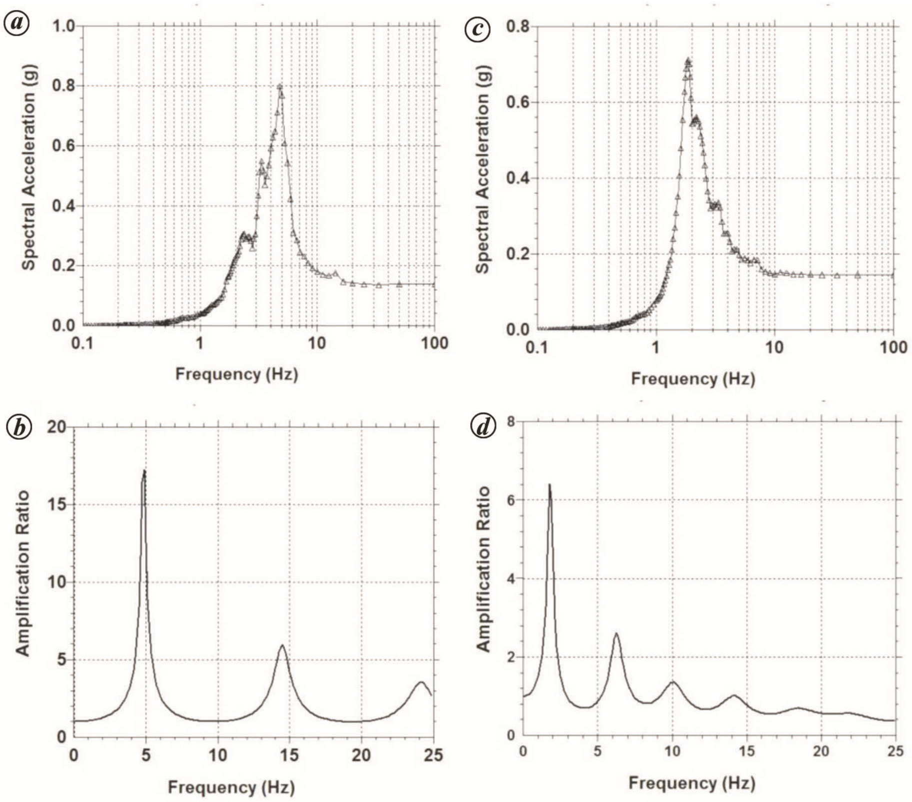

Figure 14. (***a***) Response spectrum and (***b***) amplification spectrum of Kandoli site (site no. 39) where the sediments are very thin compared to the Rajewala site (site no. 49). (***c***, ***d***) Response spectrum (***c***) and amplification spectrum (***d***) having thick sedimentary cover with very low shear wave velocity.

input parameter to obtain the response spectra for different sites of the Donga Fan, as no other strong motion data are available from the Himalayan region for any major or great earthquake. Therefore, the strong motion data of Chamoli earthquake recorded at Tehri at bedrock level was considered as the reference input motion, and the acceleration-time history has been derived at each reference site (Kandoli site; Figure 13). If needed, the shear wave velocity data can be used by other researchers for simulating the strong motion data for great earthquakes and calculate the response.

Three to four soil layers model, such as surface clay, rock fill (pebble, cobble, sticky clay sand mixed with lime) gravel, and compact gravel and boulder equivalent of rock has been considered up to 30 m, based on the exposed litho-sections and litholog information. The damping and modulus curve values were obtained from SHAKE2000 using standard values of these layers[30–34].

The SHAKE2000 software was used to calculate response analysis using various parameters like $G_{\max}$, γ_{Max}, unit weight, sub-layer thickness, damping, shear modulus curves to derive shear strain, $G_{\max}$, sub-layer thickness and damping ratios using shear wave velocity from experimental data[30–34]. The amplification spectra, response spectra along with natural frequency, average shear wave velocity of the top 30 m soil columns were derived between the free surface and the lowermost layer with infinite depth (half-space) for different damping ratios, i.e. 0.03, 0.05, 0.1 and 0.2 at each site. All response parameters were added to the attribute table to process the data in GIS format.

All point-source information was interpolated using a grid spacing of 25×25 m by considering average distance between points and the survey profile line. The interpolation technique has been used with natural grouping of data to produce several classes randomly.

Output of site response analyses

Figure 14 *a* shows the response spectrum from stiffer soils, i.e. Kandoli site (site no. 39) and Figure 14 *b* shows its corresponding amplification spectrum.

The maximum peak spectral acceleration was found to be 0.8 *g* at frequency of 4.9 Hz. The corresponding amplification spectrum for the same site showed peak amplification at 4.9 Hz with typically hard-rock amplification spectrum for the next two layers. Similarly, after examining the near-surface characteristics of Rajewala site (site no. 49), the peak response was observed at 1.8 Hz with peak spectral acceleration of 0.75 *g* (Figure 14 *c*). Its corresponding amplification spectrum shows peak amplification at 1.8 Hz (Figure 14 *d*).

Thus, it can be inferred that under thick sedimentary cover, one can have site amplification at lower frequency compared to hard-rock sites, where the site amplification was observed at >4 Hz. Since the study area is mainly occupied by either single or two-storey buildings, spectral analysis is shown only for these types of building. The spectral acceleration computed for two-storey buildings also varied from 0.19 to 0.40 *g* (at 5 Hz with 5% damping, Figure 15 *a*). Whereas, in case of single-storey buildings, spectral acceleration varied from 0.12 to 0.22 *g* (at 10 Hz with 5% damping, Figure 15 *b*). The corresponding amplification ratio varied from 6 to 15 times in the entire Donga Fan. The characteristic site periods for 30 m soil column showed variation from 0.82 to >1.00 s (1.22–1 Hz) in the south-western part of the Fan, to 0.20–0.57 s (1.75–5 Hz) in the northern part of the Fan (Figure 16 and Table 1).

The central part of the Fan showed a variation in site characteristics from 0.60 to 0.70 s (1.66–1.42 Hz). According to the horizontal to vertical spectral ratio (HVSR) studies from Doon Valley[35], the predominant frequency obtained in the Fan ranged from 0.13 to 2 Hz in the southern part, 2.5 to 4 Hz in the central part, and 5 to 8 Hz in the northern part, which is in good agreement with the peak spectral frequency obtained in the present study (Table 1).

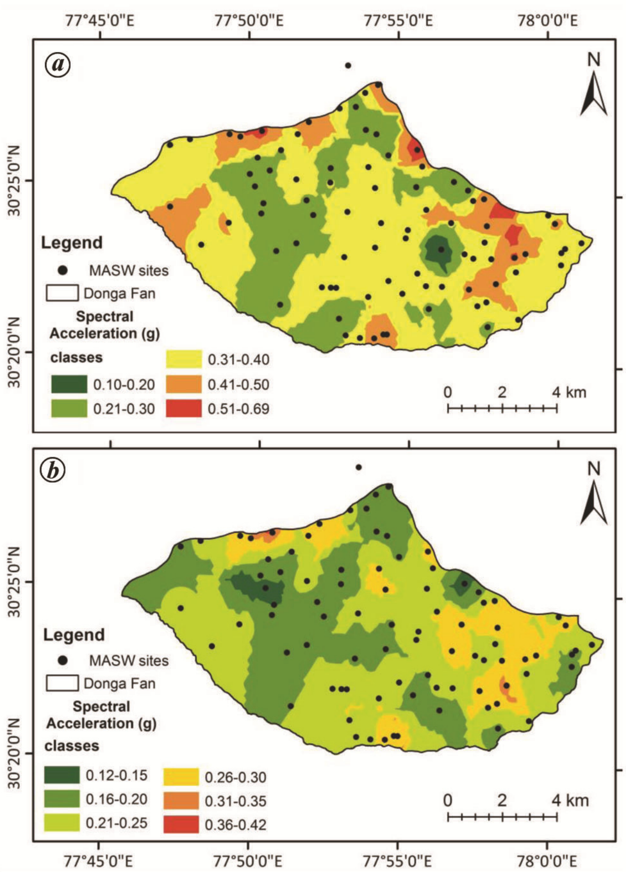

Figure 15. ***a***, Spectral acceleration map of the Donga Fan at 5% damping level considering two storey building structures (natural frequency = 5 Hz). ***b***, Spectral acceleration map of the Donga Fan at 10% damping level considering single-storey building structures (natural frequency = 10 Hz).

Conclusion

Given the lack of knowledge on the recurrence interval for major or great earthquakes in the Himalayan region, the reconciliation of site amplification using geotechnical properties of the near surface is of utmost importance. Further, the construction of any engineering site is dependent on the understanding of the subsurface information, i.e. stiffness parameters of the soil column and their effect on the buildings during strong excitation. V_s profile is one of the key parameters in this respect and can provide a relative means of determining environmental effect of the subsurface. The assessment of site-effect studies at micro-scale or urban-level scale requires knowledge of elastic properties of subsoil down to bedrock level to estimate bedrock motion expected at the site[35].

As the construction of any engineering site is dependent on the understanding of the near-surface properties of the material, therefore stiffness parameters of the soil column and their effect on the buildings during strong excitation have been estimated. In the present study, variation of shear wave velocity in the top 30 m soil column has been derived using MASW method. The study reveals that majority of the Donga Fan area comes under soil class D (V_s 180–360 m/s) according to NEHRP classification. The spatial distribution of V_s has provided valuable information on the stiffness of the soil in different parts of the Fan area. The characteristic site period of each site computed using response analysis is in good agreement with the fundamental frequencies derived using the HVSR technique[35]. The northern part of the

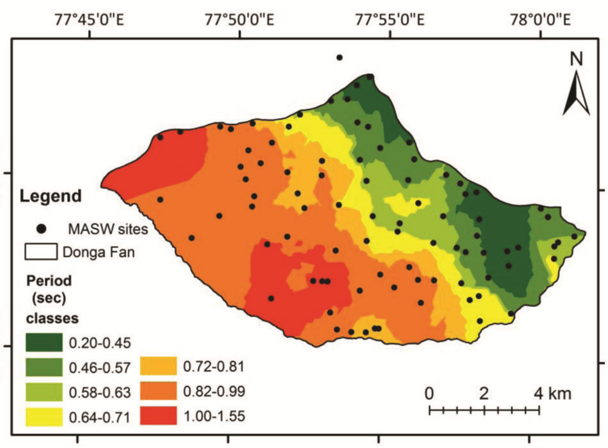

Figure 16. Variation in characteristic site period over the Donga Fan, which is in good agreement with the results obtained using microtremor analysis[19,20].

Table 1. Various response parameters using SHAKE2000 analysis

Site no.	Site name	Bedrock depth	Period (T)	PGA (g)	V_s Bedrock (Ft/s)	V_s Bedrock (mt/s)	PSA		SA at 5% damp			PAR	
							Accel.	Freq.	5 Hz	1 Hz	10 Hz	Ratio	Freq.
1	Tauli Langha	36	0.50	0.2070	952	288	0.95	2.32	0.29	0.08	0.22	8.16	2.12
2	NT59 (Pipalsar Vill)	19	0.20	0.143	1248	378	0.6705	4.76	0.630	0.039	0.174	14.37	5
3	GIC Langha	30	0.35	0.186	1121	340	1.08	2.85	0.286	0.062	0.195	9.23	2.87
4	Kotra Kalyan-pur	25	0.24	0.187	1377	417	1.09	4.34	0.698	0.040	0.248	18.00	4.62
5	Donga	42	0.67	0.109	826	250	0.490	1.61	0.200	0.088	0.119	8.58	1.5
6	NT40	50	0.49	0.144	1355	411	0.787	1.81	0.197	0.080	0.168	8.56	1.75
7	NT56	50	0.67	0.220	986	299	0.864	1.78	0.387	0.094	0.251	9.39	1.62
8	Bidholi	23	0.25	0.231	1219	369	1.10	4.16	0.550	0.041	0.266	10.69	4
9	NT14 (Dhaulas)	30	0.45	0.197	876	265	1.07	2.38	0.293	0.079	0.212	7.40	2.25
10	Dhauals Chauki	25	0.31	0.264	1088	330	1.48	3.22	0.461	0.045	0.305	8.67	3.25
11	NT45	49	0.52	0.210	1251	379	0.90	2.27	0.301	0.084	0.223	8.92	2
12	NT27 (Tikri)	62	0.63	0.134	1287	390	0.624	1.72	0.244	0.088	0.136	8.59	1.62
13	Langha	67	0.51	0.243	1721	522	1.15	2.32	0.357	0.089	0.264	11.01	2.12
14	NT26 (Barwa)	46	0.49	0.198	1231	373	0.864	2.27	0.268	0.081	0.209	8.53	2
15	NT58	49	0.57	0.160	1130	342	0.824	1.81	0.261	0.083	0.176	8.80	1.75
16	Kalyanpur	51	0.54	0.177	1243	377	0.948	1.88	0.264	0.082	0.182	8.7	1.87
17	NT50	44	0.43	0.242	1351	409	1.57	2.5	0.352	0.083	0.264	10.73	2.5
18	NT8	78	0.84	0.161	1225	371	0.727	3.22	0.233	0.150	0.181	11.17	1.25
19	NT60	39	0.32	0.278	1636	496	1.69	3.22	0.478	0.048	0.313	10.91	3.12
20	NT44	68	0.55	0.240	1643	498	1.07	1.88	0.393	0.090	0.257	9.9	2
21	Hariyawala	95	0.75	0.173	1675	508	1.00	3.22	0.320	0.111	0.185	11.08	1.37
22	NT15	102	0.76	0.179	1776	538	0.985	3.22	0.307	0.111	0.189	12.04	1.5
23	Rudarpur	76	0.57	0.246	1768	536	1.24	1.88	0.441	0.095	0.264	11.60	1.87
24	Gadaria	78	0.62	0.230	1666	505	0.971	1.81	0.382	0.092	0.266	10.76	1.75
25	NT51	88	0.63	0.232	1850	561	1.07	1.81	0.385	0.093	0.265	11.93	1.75
26	NT57	117	1	0.151	1546	468	0.765	2.5	0.23	0.24	0.154	9.76	1
27	NT52	67	0.76	0.174	1479	448	0.671	3.70	0.322	0.105	0.189	11.16	1.37
28	Tilwadi	67	0.56	0.233	1566	475	1.06	1.88	0.361	0.089	0.246	9.77	2
29	NT61	110	0.89	0.174	1645	498	0.818	3.33	0.316	0.203	0.208	9.67	1.12
30	Berowala	71	0.56	0.246	1660	503	1.09	1.88	0.415	0.091	0.266	10.28	2
31	NT9	62	0.56	0.182	1461	443	0.928	1.81	0.311	0.085	0.201	8.97	1.75
32	Kothari	67	0.58	0.232	1511	458	1.13	1.88	0.400	0.092	0.249	10.36	1.87
33	Badowala	79	0.59	0.196	1554	471	0.906	1.81	0.354	0.089	0.226	9.82	1.75
34	Bhauwala	79	0.66	0.163	1575	477	0.673	1.56	0.325	0.094	0.197	9.82	1.5
35	NT39	64	0.57	0.263	1492	452	1.14	1.88	0.105	0.096	0.288	10.83	2
36	DPS Kandoli	75	0.58	0.196	1708	518	1.02	1.85	0.318	0.086	0.206	9.29	1.87
37	Kaaswali	79	0.62	0.205	1677	508	0.782	1.75	0.337	0.093	0.242	10.62	1.62
38	NT21 (Trench Site)	68	0.59	0.207	1529	463	1.09	1.88	0.356	0.087	0.222	10.18	1.87
39	Kandoli	49	0.37	0.229	1740	527	1.44	2.94	0.375	0.062	0.265	12.64	2.87
40	Majhaun	38	0.24	0.240	2086	632	1.35	4.34	0.620	0.040	0.298	15.90	4.37
41	NT43	35	0.25	0.171	1872	567	0.957	2.94	0.251	0.059	0.188	8.12	2.87
42	NT17	86	0.68	0.185	1661	503	0.646	1.56	0.317	0.100	0.202	11.43	1.5
43	NT3 (Rudarpur Forest)	96	0.72	0.329	1756	532	1.39	3.33	0.603	0.116	0.381	12.80	1.62
44	NT55	90	0.84	0.173	1421	431	0.810	3.33	0.288	0.156	0.192	10.65	1.25
45	Chandpur Khurd	87	0.68	0.226	1680	509	1.01	3.33	0.398	0.109	0.253	11.05	1.5
46	NT49	95	0.77	0.125	1636	496	0.507	4.16	0.259	0.141	0.145	9.42	1.37
47	NT62	78	0.71	0.183	1455	441	0.686	1.56	0.291	0.101	0.199	12.08	1.5
48	Bhagwanpur	102	0.74	0.176	1818	551	1.04	3.22	0.336	0.114	0.189	11.73	1.3
49	Rajawala	130	1.13	0.159	1519	460	0.818	2.38	0.292	0.260	0.178	9.56	1
50	NT36	71	0.71	0.204	1309	397	0.750	1.72	0.386	0.098	0.233	9.94	1.62
51	NT29	111	0.79	0.180	1861	564	1.05	3.22	0.344	0.125	0.195	13.85	1.37
52	Manduwala	121	0.92	0.196	1732	525	0.977	3.33	0.369	0.201	0.218	11.03	1.25

(*Contd*)

Table 1. (*Contd*)

Site no.	Site name	Bedrock depth	Period (T)	PGA (g)	V_s Bedrock (Ft/s)	V_s Bedrock (mt/s)	PSA		SA at 5% damp			PAR	
							Accel.	Freq.	5 Hz	1 Hz	10 Hz	Ratio	Freq.
53	Dhakoliwala	98	0.81	0.187	1608	487	0.889	3.22	0.294	0.155	0.213	11.12	1.25
54	NT2	77	0.64	0.227	1592	482	0.775	1.75	0.420	0.096	0.271	10.83	1.62
55	Paundha	87	0.63	0.289	1819	551	0.688	1.72	0.480	0.094	0.332	12.23	1.62
56	Silver Heights	73	0.61	0.232	1581	479	0.880	1.75	0.363	0.093	0.288	10.10	1.62
57	NT1	81	0.61	0.220	1763	534	1.11	1.85	0.360	0.092	0.232	10.71	1.75
58	NT13 (Masandawala)	75	0.58	0.244	1711	518	1.24	1.88	0.413	0.093	0.259	9.96	2.5
59	Kedarwala Forest	116	0.98	0.189	1562	473	0.972	2.38	0.361	0.253	0.215	11.17	1.12
60	Kedarwala	89	0.71	0.271	1648	499	1.06	3.33	0.492	0.109	0.316	12.28	1.6
61	NT46	121	0.94	0.192	1696	514	0.933	2.56	0.306	0.237	0.200	11.63	1.12
62	Horawala Forest	150	1.24	0.139	1602	485	0.616	2.32	0.262	0.178	0.151	11.46	.875
63	Chhorba	121	0.99	0.145	1622	492	0.692	2.56	0.217	0.233	0.149	9.36	1
64	NT47	110	0.83	0.126	1744	528	0.566	3.22	0.213	0.200	0.134	9.31	1.12
65	NT54	123	0.83	0.143	1962	595	0.634	2.94	0.190	0.210	0.143	10.12	1.1
66	NT48	137	1.01	0.169	1783	540	0.812	2.38	0.216	0.258	0.179	10.53	1
67	NT7 (Kainchiwala)	132	1.02	0.170	1698	515	0.851	2.38	0.283	0.265	0.187	10.19	1
68	NT6	155	1.19	0.150	1722	522	0.627	2.22	0.276	0.266	0.166	9.65	.875
69	Bahadarpur	132	1	0.209	1742	528	1.06	2.5	0.325	0.260	0.215	11.45	1.12
70	NT38	106	0.80	0.195	1742	528	1.17	3.33	0.393	0.124	0.219	13.62	1.37
71	NT34	141	1.03	0.219	1815	550	1.12	2.38	0.392	0.269	0.248	10.28	1.12
72	Dhoolkot	165	1.19	0.205	1834	556	0.794	3.33	0.327	0.250	0.230	11.79	.875
73	NT30	135	1.13	0.150	1570	476	0.694	2.38	0.291	0.268	0.167	8.66	.875
74	NT28	132	0.99	0.158	1753	531	0.766	2.56	0.268	0.269	0.167	13.35	1.12
75	Kotra Santaur	104	0.95	0.153	1537	466	0.679	3.22	0.261	0.204	0.172	10.14	1.25
76	Baluwala	160	1.2	0.192	1758	533	0.864	3.33	0.337	0.305	0.216	9.99	1
77	Lakshmipur	206	1.55	0.164	1750	530	0.598	3.33	0.286	0.131	0.179	11.98	.75
78	Charba Brick Site	99	0.79	0.192	1653	501	1.18	3.33	0.425	0.129	0.216	13.67	1.37
79	Sahaspur Forest Area	103	0.77	0.201	1762	534	1.19	3.22	0.409	0.125	0.216	12.12	1.5
80	GRIC Sahaspur	108	0.84	0.192	1691	512	0.983	3.22	0.365	0.168	0.211	11.23	1.25
81	ICFAI Institute	127	0.98	0.173	1709	518	0.945	2.38	0.275	0.247	0.195	8.94	1.12
82	NT35	144	1.22	0.141	1558	472	0.609	2.27	0.157	0.212	0.264	14.17	.875
83	Bansiwala Brick Site	80	0.95	0.191	1857	563	0.911	2.56	0.335	0.224	0.197	10.57	1.12
84	Bansiwala	80	0.70	0.175	1515	459	0.677	1.56	0.300	0.099	0.194	12.22	1.5
85	Jhajra	88	0.7	0.364	1648	499	1.5	3.33	0.663	0.120	0.418	14.74	1.62
86	NT32	99	0.81	0.185	1602	485	0.874	3.22	0.308	0.154	0.213	10.00	1.25
87	NT31	91	0.68	0.236	1766	535	0.875	1.72	0.433	0.102	0.272	12.28	1.62

Donga Fan area reflects the effect of impedance contrast because of the high V_s variation between the top soft soil and the stiffer material below, whereas the southern part of the Fan shows high amplification due to greater thickness of sediments above engineering bedrock level.

The Donga Fan is characterized by long-term weathering and erosion history with unknown sediment thickness that may lead to large variation in site amplification. The present study shows variation in the stiffness of the sediments with depth, spectral acceleration and characteristic site period at different sites of the Donga Fan based on actual shear wave velocity measurements and response analysis following few assumptions. Considering the intensity variations from the past earthquakes (1905 Kangra, 1991 Uttarakashi and 1999 Chamoli), the present study will be helpful in land-use planning of the upcoming urban centre and to reduce disaster risk in the future. The present methodology will be useful for researchers studying other such valleys or duns.

1. Thakur, V. C. and Pandey, A. K., Late Quaternary tectonic evolution of Dun in fault bend/propagated fold system, Garhwal Sub-Himalaya. *Curr. Sci.*, 2004, **87**, 1567–1576.
2. BIS, Code 1893. Earthquake hazard zoning map of India, Bureau of Indian Standards, New Delhi, 2002; www.bis.org.in
3. Middlemiss, C. S., The Kangra Earthquake of 4 April 1905. *Mem. Geol. Surv. India*, 1910, **38**, 409.
4. Kumar, S. and Mahajan, A. K., The Uttarkashi earthquake of 20 October 1991: field observations. *Terra Nova*, 1994, **6**, 95–99.

5. Mahajan, A. K. and Virdi, N. S., Macroseismic field generated by 29 March, 1999 Chamoli earthquake and its seismotectonics. *J. Asian Earth Sci.*, 2001, **19**, 507–516.
6. Mahajan, A. K., Thakur, V. C., Sharma, M. L. and Chauhan, M., Probabilistic seismic hazard map of NW Himalaya and its adjoining area, India. *Nat. Hazards*, 2010, **53**, 443–457.
7. Philip, G. and Sah, M. P., Geomorphic signatures of active tectonics in the Trans-Yamuna segment of the western Doon Valley, northwest Himalaya, India. *Int. J. Appl. Earth Obs. Geo-Inf.*, 1999, **1**, 54–63.
8. Wesnousky, S. G., Kumar, S., Mohindra, R. and Thakur, V. C., Uplift and convergence along the Himalayan Frontal Thrust of India. *Tectonics*, 2000, **18**, 967–976.
9. Malik, J. N., Naik, S. P., Sahoo, S., Okumura, K. and Mohanty, A., Paleoseismic evidence of the 1505 CE (?) and 1803 CE earthquakes from the foothill zone of the Kumaon Himalaya along the Himalayan frontal thrust (HFT), India. *Tectonophysics*, 2017, **714–715**, 133–145.
10. Srivastava, H. N., Verma, M., Bansal, B. K. and Sutar, A. K., Discriminatory characteristics of seismic gaps in Himalaya. *Geomat. Nat. Hazards Risk*, 2015, **6**, 224–242.
11. Valdiya, K. S., Himalayan transverse faults and folds and their parallelism with subsurface structures of north Indian plains. *Tectonophysics*, 1976, **32**, 353–386.
12. Gahalaut, V. K. and Arora, B. R., Segmentation of seismicity along the Himalayan arc due to structural heterogeneities in the under thrusting Indian Plate and overriding Himalayan wedge. *Episode*, 2012, **35**(4), 493–500.
13. Bungum, H., Lindholm, C. D. and Mahajan, A. K., Earthquake recurrence in NW and central Himalaya. *J. Asian Earth Sci.*, 2017, **138**, 25–37.
14. Aki, K., Local site effects on weak and strong ground motion. *Tectonophysics*, 1993, **218**, 93–111.
15. Kumar, S., Wenousky, S. G., Jayangondaperumal, R., Nakata, T., Kumahara, Y. and Singh, V., Paleoseismological evidence of surface faulting along the northeastern Himalayan Front, India: timing, size, and spatial extent of great earthquakes. *J. Geophys. Res.*, 2010, **115**, B12422; https://doi.org/10.1029/2009JB006789.
16. Borcherdt, R. D., Effects of local geology on ground motion near San Francisco Bay. *Bull. Seismol. Soc. Am.*, 1970, **60**, 29–61.
17. Kramer, S. L., *Geotechnical Earthquake Engineering*, Prentice Hall, New Jersey, USA, 1996, p. 653.
18. Xia, J., Miller, R. D. and Park, C. B., Estimation of near-surface shear-wave velocity by inversion of Rayleigh waves. *Geophysics*, 1999, **64**, 691–700.
19. Mahajan, A. K., Sporry, R. J., Champati Ray, P. K., Ranjan, R., Slob, S. and Western, C. J., Methodology for site response studies using multichannel analysis of surface wave (MASW) technique in Dehradun city. *Curr. Sci.*, 2007, **92**, 945–955.
20. Mahajan, A. K. and Rai, N., Using MASW to map depth to bedrock underneath Dehradun Fan deposits in NW Himalaya. *Curr. Sci*., 2011, **100**, 233–238.
21. Thakur, V. C., Geology of Dun Valley, Garhwal Himalaya: neotectonics and coeval deposition with fault-propagation folds. *J. Himalayan Geol.*, 1995, **6**, 1–8.
22. Park, C. B., Miller, R. D. and Xia, J., Multichannel analysis of surface waves. *Geophysics*, 1999, **64**, 800–808.
23. Xia, J., Miller, R. D. and Park, C. B., Estimation of near surface shear wave velocity by inversion of wave. *Geophysics*, 1999, **64**, 691–700.
24. Taipodia, J., Dey, A. and Baglari, D., Influence of data acquisition and signal preprocessing parameters on the resolution of dispersion image from active MASW survey. *J. Geophys. Eng.*, 2018, **15**, 1310–1326.
25. Sheriff, R. E., *Encyclopaedic Dictionary of Exploration Geophysics*, Society of Exploration Geophysics, 1991.
26. Singh, A. K., Parkash, B., Mohindra, R., Thomas, J. V. and Singhvi, A. K., Quaternary alluvial fan sedimentation in the Dehradun Valley piggyback basin, NW Himalaya: tectonic and palaeoclimatic implications. *Basin Res.*, 2001, **13**, 449–471.
27. Street, R., Woolery, E. W., Wang, Z. and Harris, J. B., NEHRP soil classifications for estimating site-dependent seismic coefficients in the Upper Mississippi Embayment. *Eng. Geol.*, 2001, **62**, 123–135.
28. Mahajan, A. K., Applications of two-dimensional seismic tomography for subsurface cavity and dissolution features detection under Doon valley, NW Himalaya. *Curr. Sci*., 2018, **115**(5), 962–969.
29. Ordonez, G., SHAKE 2000: a computer program for the 1D analysis of geotechnical earthquake engineering problems. Earthquake Engineering Research Centre, University of California, Berkeley, USA, 2002; www.shake2000.com
30. Seed, H. B. and Idriss, I. M., Soil moduli and damping factors for dynamic response analysis. Report, University of California, Berkeley, USA, December 1970; file:///C:/Users/Lenovo/Downloads/PB197869.pdf
31. Seed, H. B., Wong, R. T., Idriss, I. M. and Tokimatsu, K., Moduli and damping factors for dynamic analyses of cohesionless soils. *J. Geotech. Eng.*, 1986, **112**, 1016–1032.
32. Sun, J. I., Golesorkhi, R. and Seed, H. B., Dynamic moduli and damping ratios for cohesive soils. Earthquake Engineering Research Report 81, University of California, Berkeley, USA, 1988; https://nehrpsearch.nist.gov/static/files/NSF/PB91210922.pdf
33. Gazetas, G. and Dakoulas, P., Seismic analysis and design of rockfill dams: state-of-the-art. *Soil Dyn. Earthq. Eng.*, 1992, **11**, 27–61.
34. Vucetic, M. and Dobry, R., Effect of soil plasticity on cyclic response. *J. Geotech. Eng.*, 1991, **117**, 89–107.
35. Mundepi, A. K., Seismic microzonation study in Doon Valley, Northwest Himalaya, India. *Geol. J. Soc.*, 2013, **81**, 767–773.

ACKNOWLEDGEMENTS. We thank Wadia Institute of Himalayan Geology, Dehradun for logistic support to carry out the survey. We also thank the Central University of Himachal Pradesh, Dharamshala for providing the necessary facilities for this study.

Received 24 October 2019; revised accepted 21 October 2020

doi: 10.18520/cs/v119/i12/1948-1960